3124 Vol. 51, No. 11 / 1 June 2026 / Optics Letters Letter

Optics Letters

High-accuracy multi-channel optical transfer delay measurement using time-gated phase-based ranging

Ting Qing,[1] Shupeng Li,[2] Zongxin Xu,[2] Zhijian Zhang,[1] and Shilong Pan[1,*]

[1] National Key Laboratory of Microwave Photonics, Nanjing University of Aeronautics and Astronautics, Nanjing 210016, China
[2] Suzhou LiuYaoSi Information Technologies Co., Ltd., Suzhou, 215500, China
*pans@nuaa.edu.cn

Received 30 March 2026; revised 8 May 2026; accepted 8 May 2026; posted 8 May 2026; published 22 May 2026

Accurate measurement of optical transfer delay (OTD) in multiple channels is crucial for applications such as optical phased array antennas, distributed fiber-optic sensors, and high-capacity multichannel optical communications. However, conventional high-accuracy microwave photonic phase-derived measurement techniques are limited to single-channel operation, where multi-channel measurements are typically performed sequentially via optical switching, resulting in low measurement efficiency. In this paper, we propose and experimentally demonstrate a high-accuracy, parallel multi-channel OTD measurement technique based on time-gated phase-based ranging. Wavelength division multiplexing (WDM) is employed to distribute multi-wavelength probe signals to multiple channels. Each wavelength corresponds to a specific channel, enabling parallel excitation and single-receiver detection, which significantly simplifies the system architecture. Although reflections from multiple channels overlap in the frequency domain, the proposed method separates individual channel responses in the time domain. The phase response of each channel is then retrieved via time-domain gating and frequency-domain processing, allowing high-accuracy delay extraction through the linear slope of the unwrapped phase. Experimental results demonstrate simultaneous parallel measurement of 8 channels with a measurement precision of ±0.25 ps. Featuring a simple architecture, high precision, and multi-channel scalability, the proposed technique provides an efficient solution for the characterization of complex optical networks and multi-core fiber systems. © 2026 Optica Publishing Group. All rights, including for text and data mining (TDM), Artificial Intelligence (AI) training, and similar technologies, are reserved.

https://doi.org/10.1364/OL.600347

Accurate optical transfer delay (OTD) measurement is indispensable for the synchronization, positioning, and characterization of modern optical systems. In recent years, it has played a vital role in applications such as optical phased array antennas, fiber-optic distributed antenna systems, multi-core fiber communications, and high-precision fiber-optic sensors [1–4]. With the rapid development of these technologies, modern optical communication systems are shifting from simple point-to-point links toward highly integrated, parallel network architectures. Consequently, there is an urgent demand to measure the OTD of multiple channels accurately, simultaneously, and efficiently. Over the past decades, numerous techniques for OTD measurement have been introduced. Traditional time-domain methods, such as optical time-domain reflectometry (OTDR) [5,6], feature a large measurement range but generally suffer from low accuracy (typically on the order of nanoseconds) limited by pulse width and sampling rates. Frequency-domain methods, such as optical frequency domain reflectometry (OFDR) [7], offer high resolution over short distances. However, their accuracy degrades significantly in long-fiber measurements due to the phase noise of the tunable laser. To achieve both a high accuracy and a large measurement range, microwave photonics (MWP)-based measurement techniques have been investigated. For example, methods based on phase-derived ranging [8], nonlinear frequency sweeping [9], and fiber-optic microwave interferometry [10] have achieved sub-picosecond accuracy and fast measurement speeds. However, the above-mentioned high-accuracy MWP-based methods [11,12] are primarily designed for single-channel measurements. If these methods are directly applied to a multi-channel system (e.g., via an optical splitter), the reflected optical signals from different channels will undergo different delays and superimpose at the photodetector. As a result, the phase noise of the optical carrier is converted into intensity noise, which severely degrades the signal-to-noise ratio (SNR) of the photocurrent. Therefore, the phase detector fails to extract the phase accurately. Conventionally, to address multi-channel measurements, optical switches must be employed to measure each channel sequentially. This approach is not only time-consuming but also introduces unpredictable delay variations (repeatability errors) from the switch itself. Alternatively, employing multiple parallel measurement setups would drastically increase the system's cost and complexity.

To address these limitations, we propose and experimentally demonstrate a parallel, multi-channel OTD measurement technique using time-gated phase-based ranging. Instead of sequential optical switching, wavelength-division multiplexing (WDM) [13] is employed to distribute a swept microwave-modulated multi-wavelength source into multiple channels, as can be seen in Fig. 1(a). The reflected signals are then multiplexed and detected by a single photodetector, enabling parallel excitation and single-receiver detection. In previous optical vector analysis (OVA) work [11,14], a low-coherence optical carrier

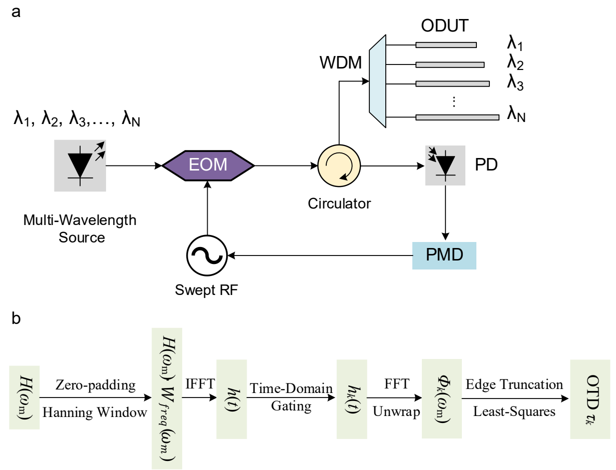

Fig. 1. (a) Schematic diagram of the proposed multi-channel optical transfer delay measurement system using time-gated phase-based ranging. EOM, electro-optic modulator; ODUT, optical device under test; PD, photodetector; PMD, phase-magnitude detector; RF, radio frequency; WDM, wavelength-division multiplexing. (b) Flowchart of the time-gated phase-based ranging algorithm.

was employed to ensure stable superposition of optical spectral responses from multiple cascaded DUTs in a single-wavelength, single-channel system. In contrast, the present work is accomplished using a multi-wavelength optical carrier and WDM to achieve the stable superposition of microwave responses from multiple parallel channels. In this case, the problem is mapped into a multi-tap microwave filter model, where each tap corresponds to a distinct channel. To address this issue, we introduce a slope-based phase extraction method that utilizes only the linear region of the unwrapped phase response after time-domain gating. By extracting the delay from the phase–frequency slope $\phi(f) = -2\pi f \tau$, the method eliminates the constant phase offsets introduced by windowing and avoids errors from conventional single-frequency phase extraction. Experimental results demonstrate the simultaneous measurement of 8 channels with a precision of ±0.25 ps. Furthermore, because the discrete optical carriers can be aligned with the ITU-T grid, this switch-free scheme can be seamlessly integrated into modern WDM networks, enabling in-service, real-time delay monitoring without disrupting data traffic.

The schematic of the proposed multi-channel optical transfer delay measurement system is illustrated in Fig. 1. A multi-wavelength optical source generates N independent continuous-wave (CW) optical carriers with different wavelengths ($\lambda_1, \lambda_2, \ldots, \lambda_N$). These optical carriers are fed into an electro-optic modulator (EOM, e.g., a Mach–Zehnder modulator) driven by a frequency-swept RF signal from a microwave source. Mathematically, the optical field at the output port of the modulator can be expressed as:

$$E_{out}(t) = \sum_{i=1}^{N} E_{c,i}[1 + M\cos(\omega_m t)]\exp(j\omega_{c,i}t), \tag{1}$$

where $E_{c,i}$ and $\omega_{c,i}$ are the amplitude and the angular frequency of the i-th optical carrier, respectively. M is the modulation index, and ω_m is the angular frequency of the swept RF signal.

The modulated multi-wavelength signal is then launched into a WDM via an optical circulator or optical coupler (OC). The WDM acts as a demultiplexer that separates different wavelengths and routes each wavelength λ_i into its corresponding channel. After propagating through the optical device under test (ODUT) in each channel, the optical signals are reflected, experiencing different optical transfer delays τ_i. The reflected signals re-enter the WDM, where they are multiplexed back into a single fiber. The total reflected optical field is given by:

$$E_{ref}(t) = \sum_{i=1}^{N} \alpha_i E_{c,i}\left[1 + M\cos\left(\omega_m\left(t - \tau_i\right)\right)\right] \cdot \exp(j\omega_{c,i}(t - \tau_i)), \tag{2}$$

where α_i represents the overall insertion loss of the i-th channel.

The multiplexed reflected signal is then sent to a photodetector (PD). Since the frequency spacing between different WDM channels is much larger than the bandwidth of the PD, the beating components between different optical carriers can be ignored. The PD only detects the intensity modulation carried by each carrier. Therefore, the recovered photocurrent is the linear superposition of the delayed microwave signals from all channels:

$$I_{RF}(t) = \sum\nolimits_{i=1}^{N} 2M\alpha_i^2 E_{c,i}^2 \cos\left(\omega_m\left(t - \tau_i\right)\right), \tag{3}$$

where η is the PD responsivity. Inter-channel crosstalk is negligible even in 64-channel DWDM scaling, as >30 dB optical isolation of standard WDM filters results in >60 dB electrical isolation due to square-law photodetection. Fiber nonlinearities are also avoided by the sub-milliwatt probe power. Although severe power imbalance can cause "strong-burying-weak" interference, channels remain resolvable if sufficiently separated in the time domain.

The phase-magnitude detector (PMD) extracts the amplitude and phase of the recovered microwave signal at the swept frequency ω_m. The measured complex frequency response of the multi-channel system can be written as:

$$H(\omega_m) = \sum\nolimits_{i=1}^{N} K_i \exp\left(-j\omega_m \tau_i\right), \tag{4}$$

where K_i is the lumped amplitude coefficient for the i-th channel, proportional to $2\eta M\alpha_i^2 E_{c,i}^2$. According to Eq. (4), the measured frequency response resembles that of a multi-tap filter. It is hard to directly extract the precise delay τ_i from the raw phase of $H(\omega_m)$.

To separate the mixed responses and achieve high-accuracy OTD measurement for each channel, a time-gated phase-based ranging algorithm is implemented. The measured complex frequency response $H(\omega_m)$ over the sweeping bandwidth from f_{start} to f_{stop} is first zero-padded to extend the frequency range down to DC. To suppress the time-domain sidelobes caused by the finite sweeping bandwidth, a windowing function (e.g., a Hanning window) $W_{\text{freq}}(\omega_m)$ is applied to the frequency response. Then, an inverse fast Fourier transform (IFFT) is performed to convert the frequency-domain data into the time domain:

$$h(t) = \text{IFFT}\{H(\omega_m) \cdot W_{\text{freq}}(\omega_m)\}, \tag{5}$$

where $B = f_{\text{stop}} - f_{\text{start}}$ is the microwave sweeping bandwidth. In the time domain, the responses of different channels are distinguished as discrete reflection impulses located at their respective delays τ_i.

It should be noted that a two-step process is required to associate each impulse with its corresponding physical channel.

First, a baseline measurement is performed without the ODUTs to determine the intrinsic delay of each WDM channel. Second, after connecting the ODUTs, prior knowledge of their approximate lengths is needed to correctly associate each newly appeared time-domain impulse with its corresponding physical path. Once this initial one-to-one mapping is established, the proposed method can be used for precise OTD measurement and continuous real-time monitoring of all channels. For established networks, this impulse-to-channel mapping is a one-time calibration; for unknown or dynamic systems, automated mapping can be readily achieved through brief sequential wavelength initialization.

To extract the precise OTD of a specific target channel (e.g., the kth channel), a time-domain gate (window) $w_k(t)$ is applied. The center of the gate is aligned with the coarse delay location $\tau_{c,k}$ observed in the time domain, and its width is chosen to encompass the main lobe of the kth impulse while rejecting the impulses from other channels. The selected time-domain response is:

$$h_k(t) = h(t) \cdot w_k(t). \quad \textbf{(6)}$$

By applying a fast Fourier transform (FFT) to the impulse response $h_k(t)$, the frequency response of the k-th channel can be obtained:

$$H_k(\omega_m) = \mathrm{FFT}\{h_k(t)\} = |H_k(\omega_m)| \exp(j\phi_k(\omega_m)), \quad \textbf{(7)}$$

where $\phi_k(\omega_m)$ is the extracted phase response. A phase unwrapping operation is executed to eliminate the 2π phase ambiguity, yielding a continuous phase variation $\phi_k(\omega_m)$.

Theoretically, the unwrapped phase $\phi_k(\omega_m)$ should exhibit a perfectly linear relationship with the microwave frequency, i.e., $\phi_k(\omega_m) = -\omega_m \tau_k$. However, the time-domain gating operation $w_k(t)$ is equivalent to a convolution in the frequency domain, which inevitably introduces nonlinear distortions (edge effects) at the boundaries of the extracted phase response (near f_{start} and f_{stop}).

To eliminate the ranging error caused by these edge effects, and to fully utilize the spectral information to suppress random phase noise, a least-squares linear regression is applied exclusively within the strictly linear region located in the central part of the frequency band. Based on the linear regression model, the precise optical transfer delay of the k-th channel is accurately determined by:

$$\tau_k = -\frac{\sum(\omega_m - \bar{\omega}_m)\varphi_k(\omega_m)}{\sum(\omega_m - \bar{\omega}_m)^2}, \quad \textbf{(8)}$$

where $\bar{\omega}_m$ is the mean angular frequency of the discrete sampled frequency points within the selected frequency range. This least-squares estimation provides an unbiased evaluation of the optical delay. It should be noted that the minimum resolvable delay spacing between adjacent channels is fundamentally constrained by the time-domain main-lobe broadening induced by the finite sweeping bandwidth and the required time-gate width to avoid phase errors.

To verify the feasibility and accuracy of the proposed multichannel optical transfer delay measurement system, an experiment based on the setup shown in Fig. 1 was performed. In the experiment, a swept microwave signal generated by a VNA with a frequency range from 10 MHz to 2 GHz was applied to modulate the multi-wavelength optical carriers. Figure 2 illustrates the raw microwave frequency response measured by

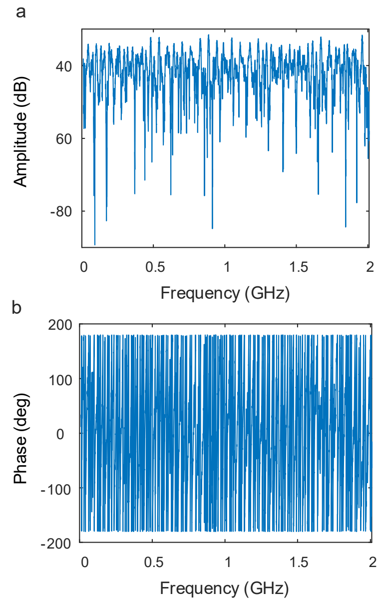

Fig. 2. Measured microwave frequency response of the multichannel system. (a) Amplitude response. (b) Phase response.

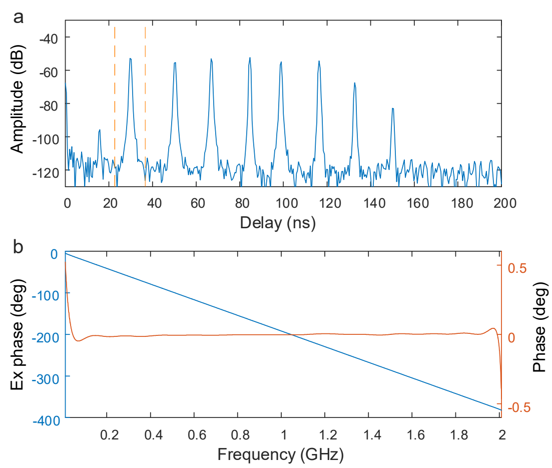

Fig. 3. Signal processing results of the time-gated phase-based ranging algorithm. (a) Time-domain reflection impulses obtained by IFFT. The dashed orange lines indicate the applied time-domain gate for selecting a target channel. (b) Extracted unwrapped phase (blue curve, left axis) and detrended phase error (orange curve, right axis) of the desired channel.

the VNA. As shown in Figs. 2(a) and 2(b), both the amplitude and phase responses exhibit significant irregular fluctuations, caused by multiple reflections. To resolve this issue, the proposed time-gated phase-based ranging algorithm was applied. First, the frequency response was zero-padded to DC, multiplied by a Hanning window, and transformed into the time domain via IFFT. As shown in Fig. 3(a), the previously irregular spectral interference is clearly resolved into distinct discrete impulses in the time domain. Each impulse represents the reflection from a specific WDM channel.

To extract the delay of the target channel (e.g., the impulse at approximately 30 ns), a time-domain gate (indicated by the dashed orange lines in Fig. 3(a)) was applied to select the desired impulse while rejecting all other reflection components.

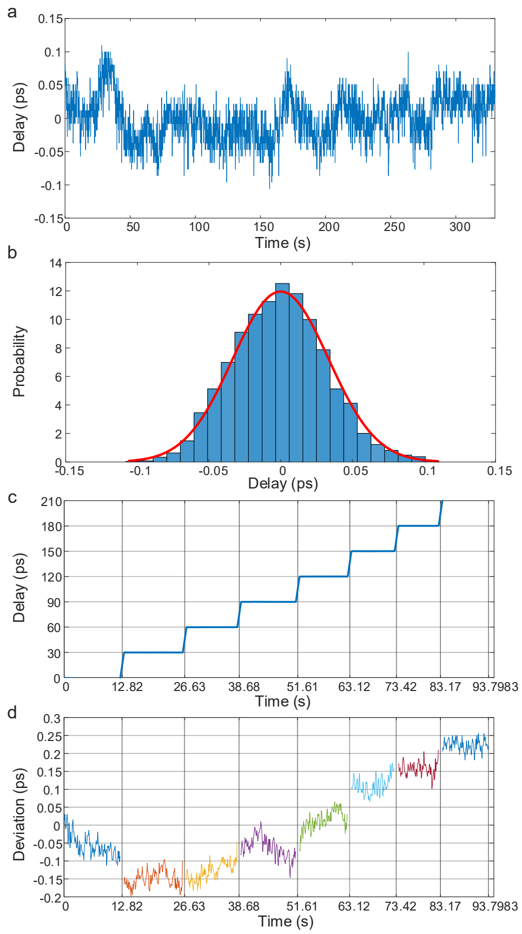

Fig. 4. Evaluation of the proposed system. (a) Delay fluctuations of a single channel over 330 s measurement. (b) Histogram and Gaussian fit of the delay fluctuations. (c) Measured OTD for 30-ps steps applied with a motorized optical delay line. (d) Deviations of the measured delays from the set delays.

The gated time-domain signal was then transformed back into the frequency domain via FFT. Figure 3(b) displays the extracted unwrapped phase of the selected channel. As expected, the extracted phase (blue curve) exhibits a highly linear relationship with the microwave frequency. It is crucial to note that the time-domain gating operation inevitably introduces spectral leakage and edge distortions in the frequency domain due to the truncation effect. To better illustrate this, the linear trend was subtracted from the unwrapped phase, and the detrended phase error is shown as the orange curve in Fig. 3(b). Significant phase fluctuations can be clearly observed at the lower and upper edges of the frequency sweep range. Therefore, to ensure high accuracy, the OTD was determined exclusively by calculating the slope of the central linear region (from 0.2 GHz to 1.8 GHz), while discarding the phase responses within 200 MHz of both edges. This procedure eliminates nonlinear edge effects and enables precise measurement of the selected channel.

To further evaluate the system, the measurement stability and accuracy were experimentally investigated. A continuous measurement of a single channel over 330 s was performed to assess the system stability. Figure 4(a) shows the measured delay fluctuations. Figure 4(b) displays the corresponding probability density distribution. The fluctuations are confined within ±0.1 ps and follow a standard Gaussian distribution. This indicates excellent short-term stability, validating the effectiveness of the least-squares linear regression in suppressing random phase noise. For accuracy verification, a motorized optical delay line was inserted into one of the test channels, and the delay was increased in steps of 30 ps from 0 to 210 ps. As shown in Fig. 4(c), the measured delay accurately tracks the applied steps. Figure 4(d) plots the measurement deviation, defined as the difference between the measured and the set delays. The maximum deviation is less than ±0.25 ps. A slight low-frequency drift is observed in the deviation curve over the 95-second measurement period, primarily due to the environmental temperature variations in the fiber link. These results confirm the sub-picosecond accuracy and high resolution of the proposed technique in a multi-channel multiplexed scenario. Notably, our parallel method achieves a precision of ±0.25 ps, which is superior to the ±0.8 ps error reported in recent multi-path OTD measurement work [14] based on adaptive filtering.

In conclusion, a parallel multi-channel OTD measurement technique using time-gated phase-based ranging is proposed and demonstrated. By combining WDM and time-domain gating, overlapped frequency responses from different channels are separated in the time domain. The independent phase response of each channel is retrieved, avoiding inter-channel crosstalk. Experimental results demonstrate that the system achieves high stability with delay fluctuations within ±0.1 ps and successfully tracks 30-ps delay steps with a maximum deviation of less than ±0.25 ps. This switch-free method can be seamlessly integrated into existing dense wavelength-division-multiplexed (DWDM) networks for in-service delay monitoring, providing an efficient and highly accurate tool for complex optical system characterization.

Funding. National Natural Science Foundation of China (62271249); Ministry of Industry and Information Technology of China (2024GX127).

Disclosures. The authors declare no conflicts of interest.

Data availability. Data underlying the results presented in this paper can be obtained from the authors upon reasonable request.

REFERENCES

1. B. Culshaw and A. Kersey, J. Lightwave Technol. **26**, 1064 (2008).
2. W. Ng, A. A. Walston, G. L. Tangonan, *et al.*, J. Lightwave Technol. **9**, 1124 (1991).
3. F. Zhang, Q. Guo, Z. Wang, *et al.*, Opt. Express **25**, 16274 (2017).
4. B. Wang, C. Gao, W. L. Chen, *et al.*, Sci. Rep. **2**, 556 (2012).
5. A. H. Hartog, M. P. Gold, and A. P. Leach, "Optical time-domain reflectometry," U.S. patent 4,823,166 (1989).
6. Y. Kim, J. Sung, S. R. Hong, *et al.*, IEEE Trans. Instrum. Meas. **57**, 947 (2008).
7. W. Eickhoff and R. Ulrich, Appl. Phys. Lett. **39**, 693 (1981).
8. S. Li, M. Xue, T. Qing, *et al.*, IEEE Photon. Technol. Lett. **31**, 1351 (2019).
9. S. Li, T. Qing, J. Fu, *et al.*, IEEE Trans. Instrum. Meas. **70**, 8000204 (2021).
10. S. Li, T. Qing, J. Fu, *et al.*, J. Lightwave Technol. **39**, 627 (2021).
11. S. Li, T. Qing, L. Wang, *et al.*, Opt. Lett. **46**, 186 (2021).
12. L. Wang, X. Wang, X. Liu, *et al.*, Photonics Res. **13**, 1302 (2025).
13. A. A. Sardarzadeh, P. Li, and J. Yao, in *International Topical Meeting on Microwave Photonics* (2024), 1–4.
14. L. Wang, L. Ren, X. Wang, *et al.*, Chin. Opt. Lett. **22**, 013901 (2024).